Lauri Närhi

TLR9 DEFICIENCY PROMOTES BONE RESORPTION AND INDUCES IL-18 EXPRESSION UPON ZOLEDRONATE TREATMENT

Syventävien opintojen kirjallinen työ

Kevätlukukausi 2022

Lauri Närhi

TLR9 DEFICIENCY PROMOTES BONE RESORPTION AND INDUCES IL-18 EXPRESSION UPON ZOLEDRONATE TREATMENT

Biolääketieteen laitos

Kevätlukukausi 2022

Vastuuhenkilö: Jouko Sandholm

TURUN YLIOPISTO
Lääketieteellinen tiedekunta

NÄRHI, LAURI: TLR9 deficiency promotes bone resorption and induces IL-18 expression upon zoledronate treatment

Syventävien opintojen kirjallinen työ, 26 s.
Solubiologia ja anatomia
Maaliskuu 2022

The aim of this study was to determine the effects of TLR9 deficiency on zoledronate-induced inflammation and bone formation. TLR9 is an intracellular DNA receptor expressed in innate immune system cells. Zoledronate is a medicine used to treat bone loss caused by osteoporosis. Zoledronate has effects on bone-resorbing osteoclasts as well as on bone-building osteoblasts. It has also been found in previous studies that zoledronate has a pro-inflammatory effect on several cytokines. TLR9 has been shown to have an influence on the effects of zoledronate, but there is very limited research on the relationship between TLR9 and zoledronate.

The data included 24 mice. 12 of these were TLR9 knockout mice that had the lack of exon 1 in TLR9 gene and did not produce functional TLR9 protein. The other 12 mice were wild type mice from the same strain. Of both groups, 6 mice were treated once a week with a dose of zoledronate, and 6 mice were treated with vehicle. The mice were euthanized after 5 weeks. Kidneys, lungs, livers, spleens, and tibiae were dissected and stained for histological analysis. Femurs were imaged with microtomography and analyzed. Blood samples were collected at sacrifice by cardiac puncture. Cytokine concentrations in plasma were analyzed with an immunoassay.

We observed that TLR9 deficiency prevented bone formation upon zoledronate treatment. We also found that TLR9 deficiency increased IL-18 expression. The role of TLR9 in N-BP-induced inflammation remains an important subject of research.

Key words: zoledronate, TLR9

ABBREVIATIONS

ABC	avidin/biotinylated enzyme complex
ASC	apoptosis-associated speck-like protein containing a caspase recruitment domain
ATP	adenosine triphosphate
BP	bisphosphonate
CpG	cytosine-phosphorothioate-guanine
DAB	3,3′-diaminobenzidine
DNA	deoxyribonucleic acid
EDTA	ethylenediaminetetraacetic acid
FPP	farnesyl diphosphate
GGPP	geranylgeranyl diphosphate
GPP	geranyl diphosphate
GTPase	guanosine triphosphatase
H&E	hematoxylin and eosin
HMG-CoA	3-hydroxy-3-methylglutaryl coenzyme A
IFN-γ	interferon gamma
IHC	immunohistochemical staining
IL	interleukin
IPP	isopentenyl diphosphate
KO	knockout
MyD88	myeloid differentiation primary response protein 88
N-BP	nitrogen-containing bisphosphonate
NLRP3	nucleotide-binding domain -like receptor protein 3
PAMP	pathogen-associated molecular pattern
RANKL	receptor activator of NF-kappaB ligand
TLR9	Toll-like receptor 9
TNFα	tumor necrosis factor alpha
TRAP	tartrate-resistant acid phosphatase
WT	wild type
Zol	zoledronate

INTRODUCTION

Toll-like receptor 9 (TLR9) is an intracellular DNA receptor expressed in innate immune system cells, such as macrophages and dendritic cells(1–3). TLR9 recognizes pathogen-associated molecular patterns (PAMPs), which are expressed on infectious agents(1). TLR9 binds DNA of invading pathogens, such as bacteria and viruses, and triggers a pro-inflammatory cytokine response, which includes production of IL-1β and IL-18(4). TLR9 is also expressed in bone cells as well as in various cancer cells(5). Cancer, tissue damage and infection can modulate TLR9 expression and activation.

The mechanism of TLR9 activation, especially in cancer, is not yet fully understood. Before stimulation, TLR9 is located in the endoplasmic reticulum of the cell(3,6). TLR9 has been shown to be activated by unmethylated CpG sequences in DNA molecules(1,2,7). However, several studies have reported CpG sequence-independent TLR9 activation by oligodeoxynucleotides or endogenous intracellular DNA as well(8–12). On stimulation with CpG DNA, TLR9 translocates to a CpG DNA -containing lysosomal compartment where it recognizes and binds to its ligand(3). Ligand binding involves interaction with MyD88, which is an adaptor protein in the signaling pathway of TLR9(3). Our research group has shown that TLR9 can be activated also without ligand-binding(13).

Bisphosphonates (BPs) are commonly used to prevent osteoporosis and bone fractures(14). They reduce bone resorption by inhibiting osteoclast activity, differentiation, and survival(14,15). Based on their molecular structure, bisphosphonates are divided into two groups: non-nitrogen-containing bisphosphonates (non-N-BPs) and nitrogen-containing bisphosphonates (N-BPs). Non-N-BPs are converted intracellularly into AppCp-type analogues of ATP(16). The AppCp-type metabolites accumulate in the cytosol of osteoclasts and other cells such as macrophages, which can internalize bisphosphonates(16,17). For instance, clodronate induces accumulation of $AppCCl_2p$, which in turn reduces the number of osteoclasts and increases osteoclast apoptosis(18).

N-BPs inhibit farnesyl diphosphate (FPP) synthase, which is an enzyme in the mevalonate pathway(19,20). The inhibition of FPP synthase results directly in prevention of FPP synthesis and indirectly in prevention of geranylgeranyl diphosphate (GGPP) synthesis(21). The lack of FPP and GGPP prevents the prenylation of small GTPases, such as Rab, Rac, and Rho, which are essential for osteoclast function(21). The prevention of prenylation, specifically geranylgeranylation, has been addressed as the mechanism explaining the effects of N-BPs(22–26). This mechanism is presented in Figure 1.

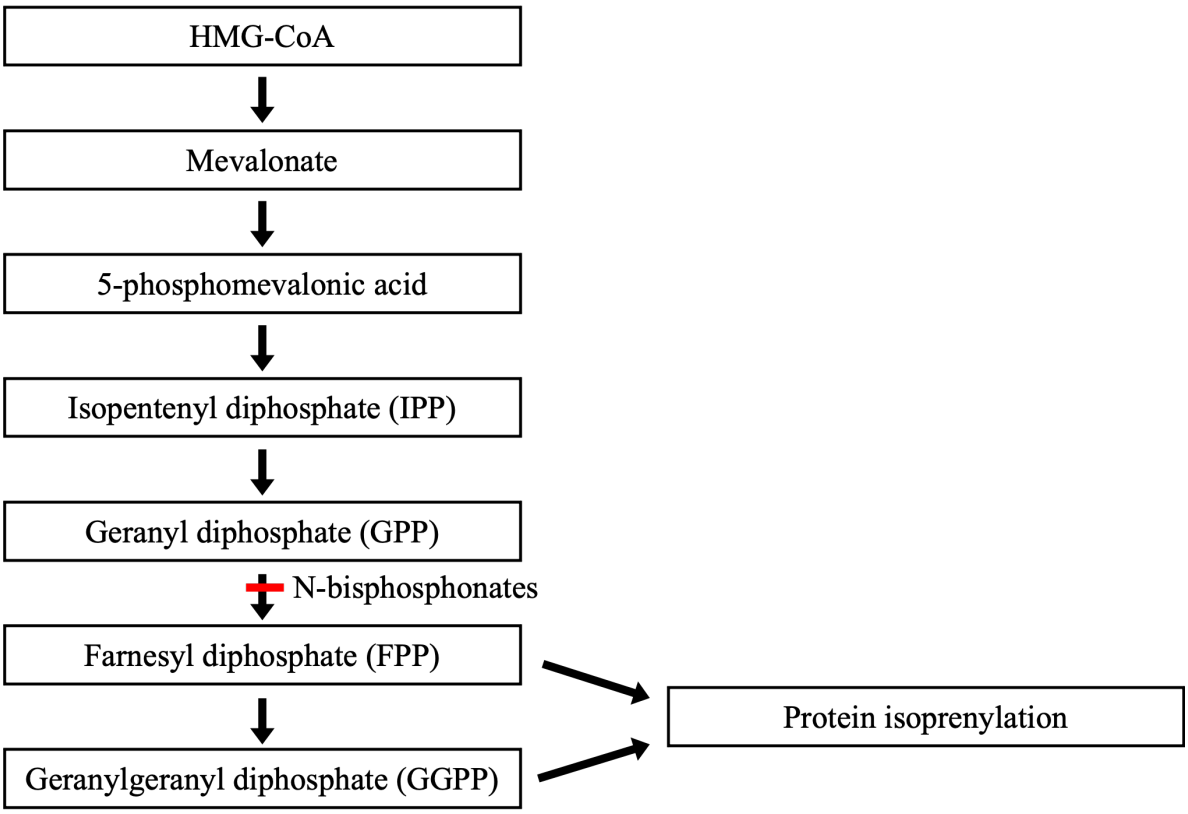

Figure 1. **The effect of N-bisphosphonates on mevalonate pathway.**(27)

N-BPs induce Caspase-1 activation, leading to the up-regulation of IL-1β and IL-18(28,29). It has been shown in several studies that N-BPs have a pro-inflammatory response involving the upregulation of cytokines IL-1β, IL-6, IL-17, IL-18, and TNFα(28–32). In addition to their effects on osteoclasts, N-BPs have been shown to have effects also on osteoblasts and osteocytes. It remains unclear whether their effect on these cells is induction of apoptosis, suppression of apoptosis, or something else. It has been shown that the N-BPs pamidronate and alendronate inhibit osteoblast growth, cause osteoblast apoptosis, and inhibit bone nodule formation in vivo(33). It has also been shown that zoledronate, alendronate, and pamidronate diminish osteoblast proliferation *in vitro*(34). In a recent study, pamidronate impaired osteoblast attachment to hydroxyapatite, leading to decreased calcification(35). Controversially, some researchers have found that N-BPs inhibit osteocytic and osteoblastic cell apoptosis *in vitro*, specifically upon glucocorticoid-induced bone loss or after microdamage of the bone(36–39).

HYPOTHESIS AND AIMS

N-BPs inhibit the mevalonate pathway, which in turns leads to absence of geranylgeraniol and release of Caspase-1. DNA released from dying cells may cause TLR9 activation, which in turn results in increased cytokine expression. Cytokines are converted into their active forms by Caspase-1. The activation of cytokines inhibits osteoclast activation.

The aims of the study were to determine the effects of TLR9 deficiency on bisphosphonate-induced bone formation and on IFN-γ, IL-10, and IL-18 concentrations in mice. We hypothesized that TLR9 deficiency decreases cytokine expression and influences bisphosphonate effects on bone.

MATERIALS AND METHODS

Animal studies

In this study, we used C57black/C6 age-matched wild type (WT) and TLR9 knockout (KO) mice (n=12/group). Animals were purchased from the Jackson laboratory (MA, USA). TLR9 KO mice had the lack of exon 1 in TLR9 gene and did not produce functional TLR9 protein.

Mice were housed in individually ventilated cages under controlled pathogen-free environmental conditions (21 °C, humidity 55 ± 5%, and lights on from 6:00 a.m. to 6:00 p.m.) with free access to water and soy-free chow (RM3 (E) soy-free, 801710, Special Diets Service). Animals were cared for in accordance with the Directives 2012/707/EU, 2014/11/EU and of the European Parliament and of the Council for the Care and Use of Laboratory Animals. License (ESAVI/2329/04.10.07/2017) was obtained from the Regional State Administrative Agencies in Finland.

The mice were randomized according to the body weight to four groups of 6 mice each: WT treated with vehicle (0.9% NaCl), WT treated with zoledronate (4μg/mouse), TLR9 KO treated with vehicle, and TLR9 KO treated with zoledronate. The mice were treated once a week with an i.p. (intraperitoneal) dose of vehicle or zoledronate. They were weighed twice a week. The mice were euthanized after 5 weeks.

Sample preparation

Kidneys, lungs, livers, and tibiae were dissected for histological analysis. All samples were processed into paraffin-embedded tissue blocks. All samples were fixed with 4% paraformaldehyde for 24 hours. Bone samples were decalcified with 10% EDTA for 14 days with a new solution every third day. Then, all samples were washed in running tap water for 2 hours, dehydrated by 70%, 95%, and 100% ethanol and xylene for 1h each at 37°C, and embedded in paraffin overnight. The samples were cut into transverse tissue sections.

Staining of kidney, liver, and lung tissues

Tissue sections were stained with hematoxylin and eosin (H&E) staining. The tissue sections were deparaffinized with the series of xylene, ethanol, and double-distilled water. Samples were stained by standard hematoxylin and eosin protocol (Delafield Hematoxylin 10’, tap water 30”,

acid alcohol 30", distilled water, eosin 1,5'). Finally, slides were dehydrated with the series of ethanol and xylene, and mounted.

Quantitative analysis of bone

Quantitative analysis of femurs was performed using a Skyscan 1072 X-ray computer tomography scanner (Bruker, Kontich, Belgium) available on the University of Turku campus. Reconstruction of cross-sectional images was performed with NRecon version 1.4 software, and data analysis was performed with CTAn version 1.9.32 software, both from Skyscan (Bruker). The parameters applied for scanning were the following: x 26.31 magnification, X-ray tube voltage 61 kV, tube current 148 μA, X-ray filtration with 0.25 mm aluminum filter. Exposure time was 3.9s per frame, and the object was rotated in steps of 0.45°, total rotation angle 182.45°. Trabecular bone morphometric region of interest was defined at metaphysis of the femur starting 11 layers (122μm) below an anatomic marker, showing lower surface of the growth plate and extending 50 layers (557μm).

Morphometric parameters included tissue volume (TV, mm^3), bone volume (BV, mm^3), trabecular number (Tb.N, 1/mm), trabecular thickness (Tb.Th, mm), and trabecular separation (Tb.Sp, mm).

Staining of bone sections

Sections from tibiae were stained with H&E staining, Masson-Goldner trichrome staining, and TRAP staining (Sigma-Aldrich Co.). In Masson-Goldner trichrome staining, four different solutions were used: Weigert hematoxylin, Ponceau-Fuchsin, Phosphotungstic acid-Orange G, and Light green. Weigert hematoxylin contained equal parts of two solutions: a solution of 1 g Hematoxylin (Gurr) and 100 ml ethanol (95%), and a solution of 4 ml ferric chloride (29%) and 1 ml diluted HCl (40% HCl diluted 1:4 with dH2O) brought to 100 ml with dH2O. Ponceau-Fuchsin solution contained two solutions: a solution of 1 g Ponceau and 100 ml dH2O, and a solution of 1 g Acid Fuchsin and 100 ml distilled water. Working solution of Ponceau-Fuchsin contained 3 parts of Ponceau solution and 1 part of Fuchsin solution, and the stock was diluted 1:5 with 0.2% acetic acid. Phosphotungstic acid-Orange G solution contained 4 g Orange G (Gurr), 8 g phosphotungstic acid (Fisher), and 200 ml dH2O. Light green solution contained 0.4 g light green, 0.2 ml acetic acid, and 100 ml dH2O. The tissue sections of tibiae were deplastified, stained in Weigert hematoxylin working solution (25 min), rinsed with distilled water, washed in running tap water, and rinsed with distilled water again. Slides were stained in Ponceau-Fuchsin working solution (17 min), rinsed 2 x 1 min in 1% acetic acid, stained in freshly filtered Orange G for 7 min, rinsed 2 x 1

min in 1% acetic acid, stained in freshly filtered light green for 20 min, and once more rinsed 2 x 1 min in 1% acetic acid. Finally, the slides were dehydrated with ethanol and xylene, and mounted.

In TRAP staining, the tissue sections of tibiae were kept in PBS in room temperature for 5 min. Slides were incubated in 0.2M Tris-HCl (pH 9.1) in +37°C for 60 min. Then, slides were incubated in 0.1M sodium acetate buffer (pH 5.0) for 5 min. Then, slides were incubated with TRAP stain (+37°C) in dark for 60 min. TRAP stain was made by mixing 150 µl Fast Garnet GBC base with 150 µl sodium nitrite, and then adding 13.5 ml ddH2O, 150 µl Naphtol AS-BI, 600 µl acetate solution, and 300 µl tartrate solution. After TRAP staining, tissue sections were washed 2 x 3 min with dH2O. Slides were incubated in Mayer Hematoxylin for 30s. After washing in tap water for 5 min, in PBS for 10s, and rinsing with distilled water, the slides were mounted.

Analysis of bone formation

Osteoclast numbers were counted per field of view in trabecular bone in H&E and TRAP stained slides. Osteoblast numbers were counted per field of view in trabecular bone in Masson-Goldner trichrome stained slides. All counts were performed with Osteomeasure (Osteometrics, Atlanta, GA, USA), using 20x magnification. Masson-Goldner's trichrome colours were separated using the Brilliant Blue option in the Color Deconvolution function of Fiji-ImageJ(40). For analysis, the bone channel image was converted into grayscale and then into a binary image, and region of interest (ROI) of the inner side of trabecular bone to the point of 2.5cm was drawn manually. ROIs were chosen following the same distance from the growth plate for each slide. The analysis was done independently by two researchers. The areas of bone formation were quantified using Fiji-ImageJ.

Cytokine measurement

Blood samples from the mice were collected at sacrifice by cardiac puncture. Plasma was separated by centrifugation (1500 x g, 10 min). Samples were stored at -80°C before cytokine measurement. Cytokine (IFN-γ, IL-18, and IL-10) concentrations were analyzed with ProcartaPlex MultiPlex immunoassay (Invitrogen, USA) according to manufacturer's instructions using the Luminex 200 system (Luminex Corporation, Austin, TX, USA). The cytokine standard range was from 0 to 10000 pg/ml. Values below detection levels were treated as 0.

Statistical methods

Continuous variables are reported with means together with standard deviation (SD) if the variable followed normal distribution and with median as well as lower and upper quantile (Q1,Q3) otherwise. Normality assumption was checked visually together with Shapiro-Wilks test. Q-Q plots were also used.

Mean values of normally distributed variables were compared between treatment groups using one-way analysis of variance (ANOVA). If statistically significant results occurred, pairwise comparison p-values were corrected with Tukey's method. Also non-parametric Kruskall-Wallis test was used together with Wilcoxon rank sum test. All statistical tests were performed as two-sided, with a significance level set at 0.05. The analyses were performed using SAS System, version 9.4 for Windows (SAS Institute Inc., Cary, NC, USA).

RESULTS

Zoledronate increased the weight of TLR9-deficient mice

Mice were weighed throughout the experiment twice a week. Zoledronate treatment did not affect animal weight in WT mice. However, zoledronate increased the weight in TLR9 KO group compared to representative untreated controls, but not significantly. The measured weights of mice are shown in Figure 2.

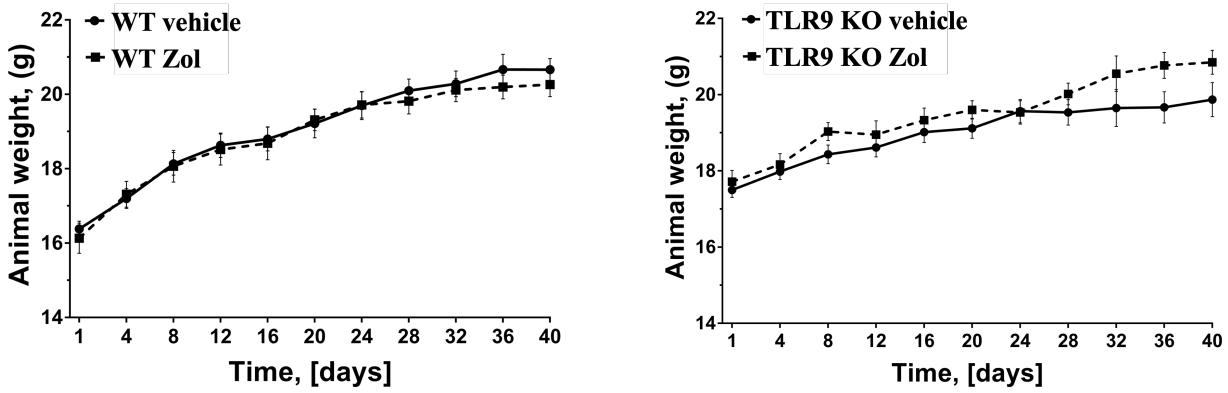

Figure 2. **Animal weights throughout the experiment**. Mice were weighed twice a week for 5 weeks.

TLR9 deficiency and zoledronate treatment did not affect cell morphology

H&E stained kidney, liver, and lung tissue sections were scanned using Pannoramic 250 slide scanner, analyzed with Pannoramic Viewer (20x and 40x magnification), and compared with each other. Representative images are presented in Figure 3. In the kidney tissue sections of WT and KO vehicle-treated groups, healthy glomeruli and kidney tubules were observed. Similar cell morphology was observed in zoledronate-treated groups. In the liver tissue sections of WT and KO vehicle-treated groups, healthy parenchyma with hepatocytes, sinusoids and some fat was observed. Stroma consisting of connective tissue could be seen. Lobular structure with hexagonal lobules and a portal canal at each corner of the lobule could be seen. Similar cell morphology was observed in zoledronate-treated groups. In the lung tissue sections of WT and KO vehicle-treated groups, healthy lung tissue with bronchioles, alveoli and blood vessels was observed. Similar cell

morphology was observed in zoledronate-treated groups. Results demonstrated that TLR9 deficiency did not change tissue morphology and that zoledronate treatment did not cause cytotoxicity.

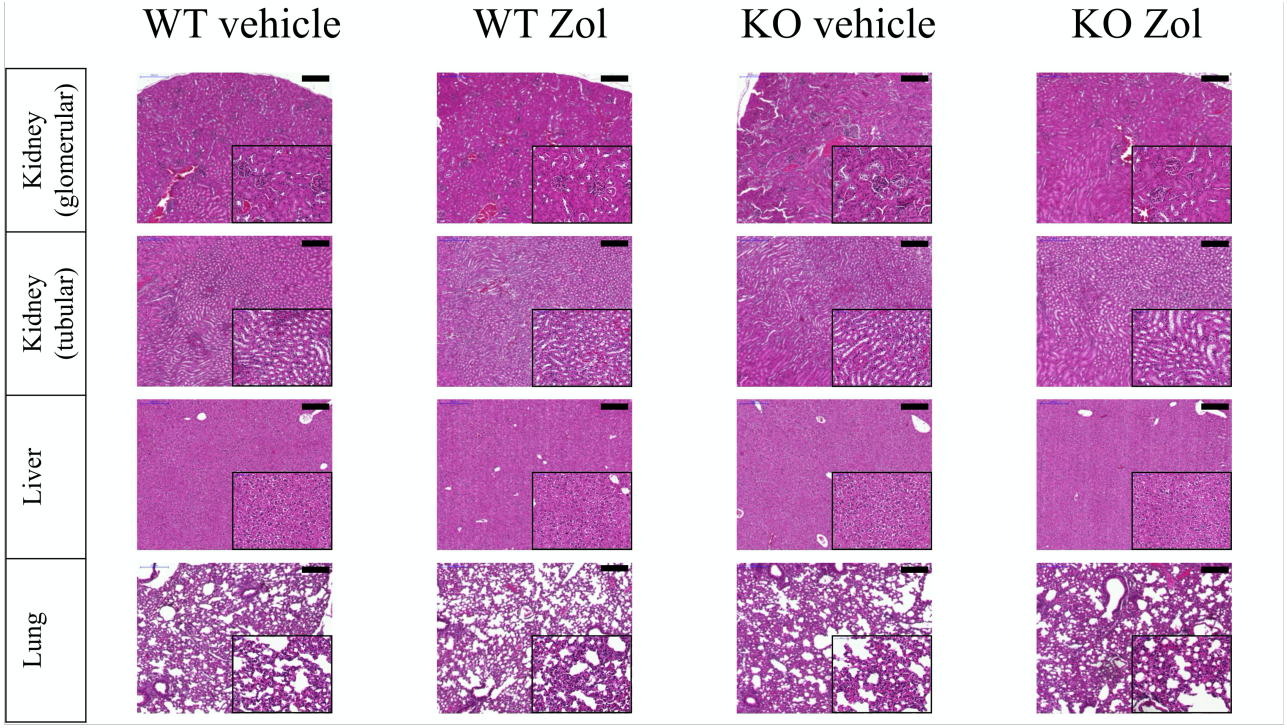

Figure 3. **The lack of TLR9 did not affect tissue morphology.** H&E stained kidney, liver, and lung tissues. 20x and 40x magnification (insets). Scale bar = 100 μm.

TLR9 deficiency and zoledronate treatment did not affect spleen weight

The spleens of mice were weighed after euthanization. Zoledronate increased spleen weight in WT and TLR9 KO groups, but not significantly. The results are shown in Figure 4.

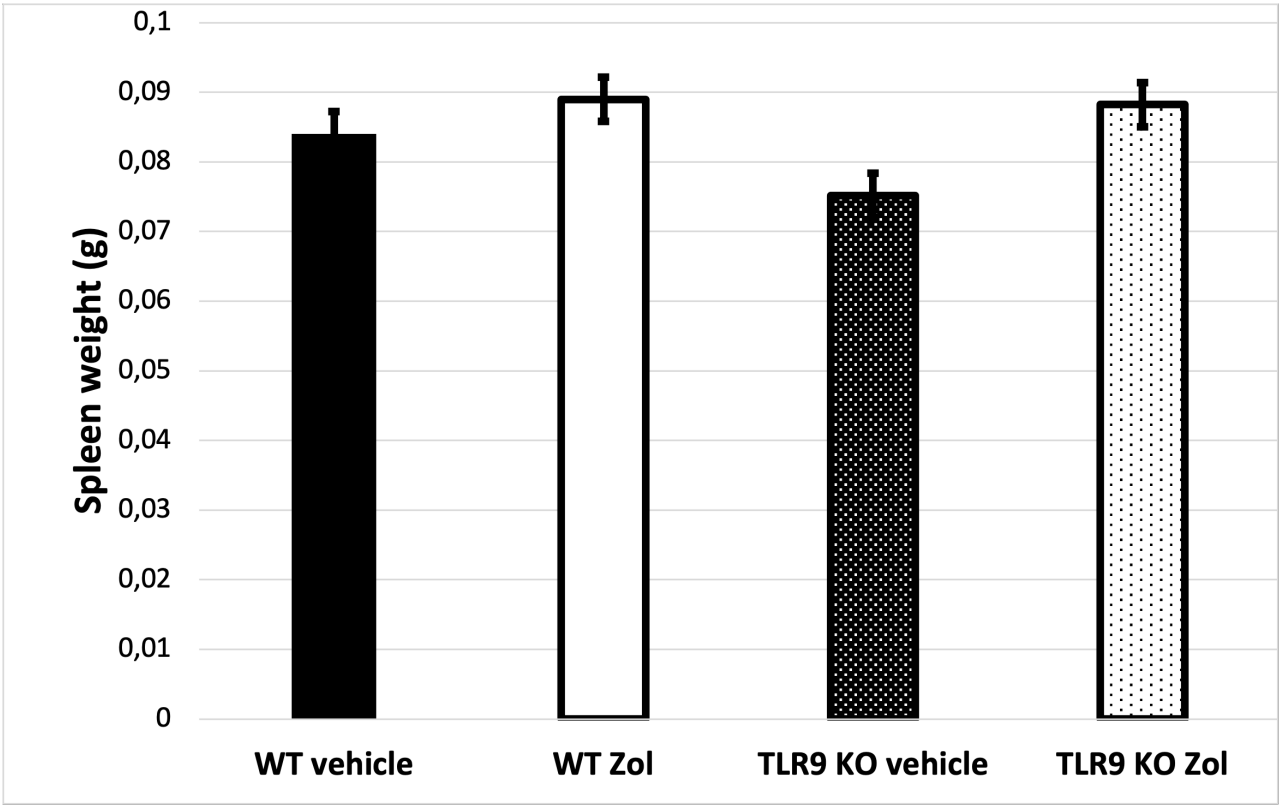

Figure 4. **Spleen weights.** The results are expressed as mean with standard error, n=6.

Effect of TLR9 deficiency on bone formation upon zoledronate treatment

To investigate whether TLR9 affected bone formation, we imaged femurs using micro-computed tomography (μ-CT), and used CTAn software for analysis.

Zoledronate significantly increased tissue volume in both WT and KO groups compared to vehicle-treated groups ($p=0.0019$). Tissue volume was significantly increased in WT zoledronate-treated group compared to TLR9 KO zoledronate-treated group ($p=0.0021$) (Fig. 5A).

Zoledronate also significantly increased bone volume in both WT and KO groups compared to vehicle-treated groups ($p=0.0206$). Bone volume was significantly increased in WT zoledronate-treated group compared to TLR9 KO zoledronate-treated group ($p=0.0329$) (Fig. 5B).

Zoledronate significantly increased bone volume fraction in both WT and KO groups compared to vehicle-treated groups ($p=0.0206$). Bone volume fraction was significantly increased in WT zoledronate-treated group compared to TLR9 KO zoledronate-treated group ($p=0.0206$) (Fig. 5C).

Additionally, zoledronate significantly increased trabecular number in both WT and KO groups compared to vehicle-treated groups ($p<0.0001$). Trabecular number was significantly increased in WT zoledronate-treated group compared to TLR9 KO zoledronate-treated group ($p=0.0001$) (Fig. 5D).

Zoledronate significantly increased trabecular thickness in both WT and KO groups compared to vehicle-treated groups ($p<0.0001$). There was no statistically significant difference between WT and KO groups upon bisphosphonate treatment (Fig. 5E).

Zoledronate significantly decreased trabecular separation in both WT and KO groups compared to vehicle-treated groups ($p<0.0001$). However, trabecular separation was statistically significantly increased in TLR9 KO zoledronate-treated group compared to WT zoledronate-treated group ($p=0.0002$). There was no statistically significant difference between vehicle-treated groups (Fig. 5F).

Taken together, the data demonstrated that zoledronate increased trabecular bone formation significantly more in WT groups than in TLR9 KO groups.

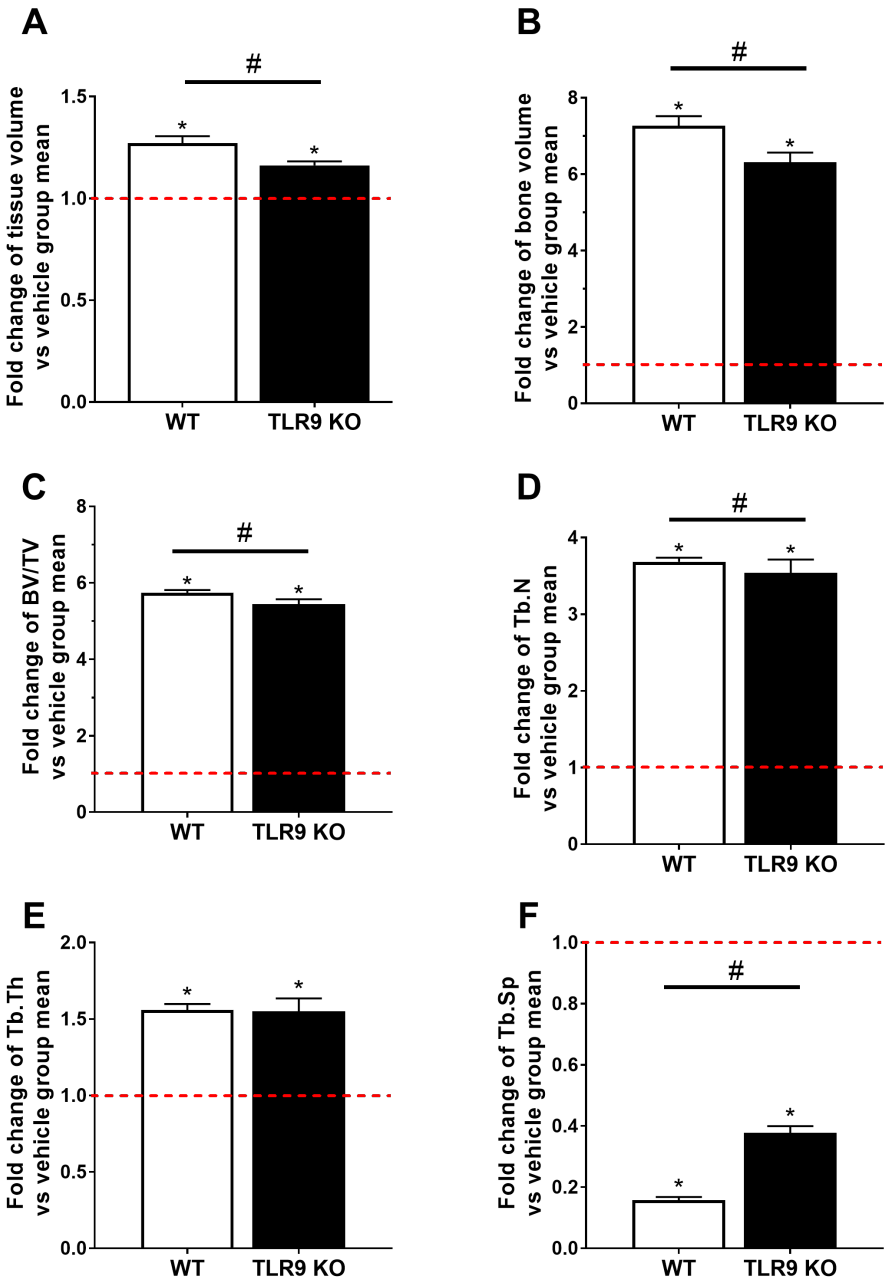

Figure 5. **Effect of zoledronate on bone formation.** (A) Tissue volume in WT and KO groups after zoledronate treatment. (B) Bone volume in WT and KO groups after zoledronate treatment. (C) Bone volume fraction in WT and KO groups after zoledronate treatment. (D) Trabecular number in WT and KO groups after zoledronate treatment. (E) Trabecular thickness in WT and KO groups after zoledronate treatment. (F) Trabecular separation in WT and KO groups after zoledronate treatment. The results are expressed as mean ± SD, n = 6. * $P < 0.05$, # $P < 0.05$ are considered to be statistically significant compared to representative control group, by Tukey's HSD (A, D, E, F) or Wilcoxon rank sum test (B,C). Dotted lines are set as 1 and express WT and TLR9 KO vehicle groups.

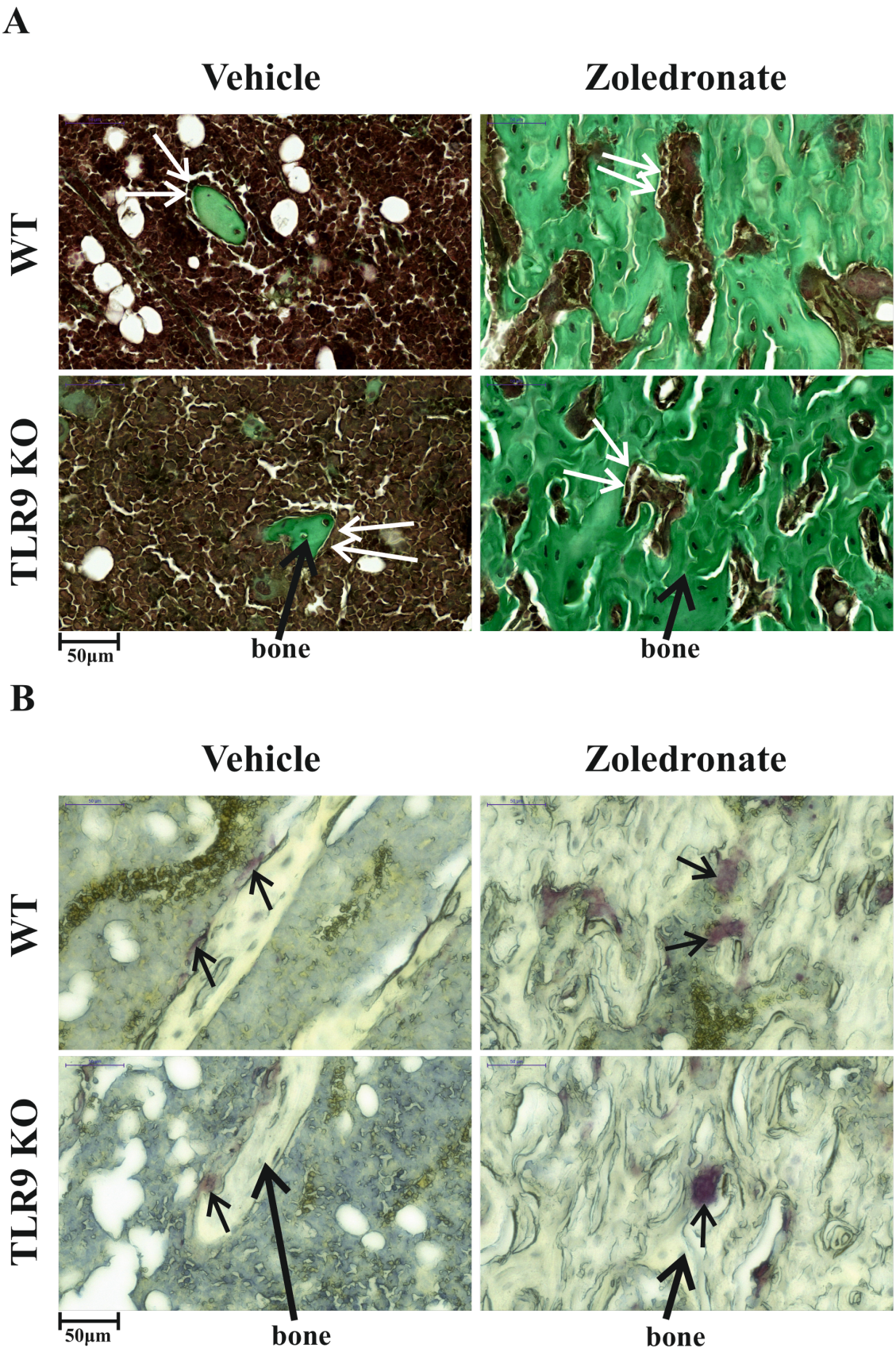

Figure 6. **Representative images of osteoblasts (A, white arrows) and osteoclasts (B, small black arrows), 40x magnification.** Scale bar = 50 µm.

TLR9 deficiency decreased number of osteoblasts upon zoledronate treatment

Next, we investigated whether TLR9 deficiency altered the effects of zoledronate on bone cells. We showed that zoledronate significantly increased the number of osteoblasts in both WT and KO groups compared to vehicle-treated groups ($p=0.0206$). Number of osteoblasts increased statistically significantly in WT zoledronate-treated group compared to TLR9 KO zoledronate-treated group ($p=0.0206$) (Fig. 7A).

Zoledronate decreased the osteoblast surface per bone surface in tibiae compared to vehicle-treated groups, but did not reach significance (Fig. 7B).

Zoledronate significantly increased the number of osteoblasts per tissue area in both WT and KO groups compared to vehicle-treated groups ($p=0.0206$). However, number of osteoblasts per tissue area was statistically significantly increased in WT zoledronate-treated group compared to TLR9 KO zoledronate-treated group ($p=0.0206$). There was no statistically significant difference between vehicle-treated groups (Fig. 7C).

Zoledronate decreased the number of osteoblasts per bone perimeter, but that did not reach statistical significance (Fig. 7D).

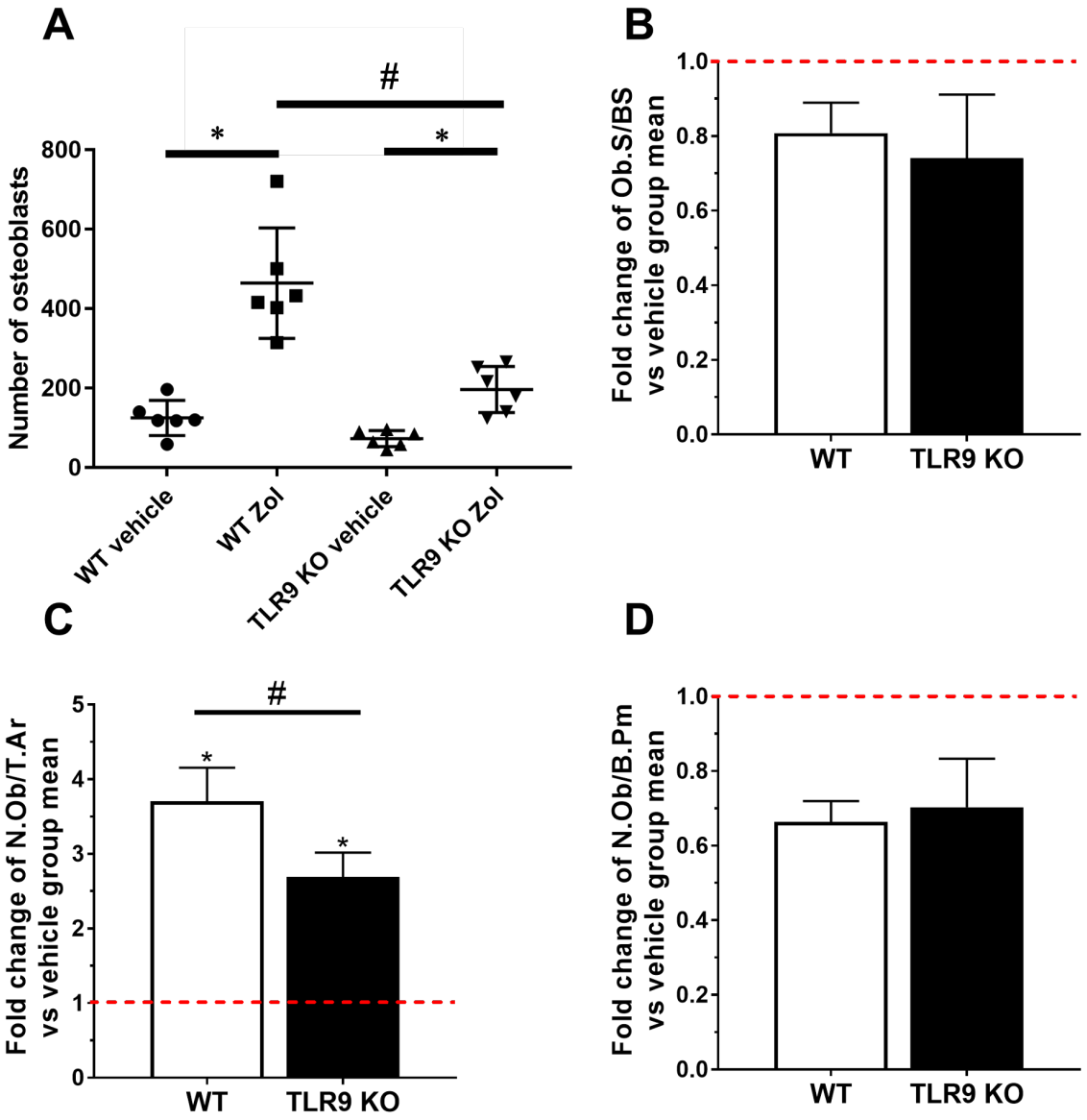

Figure 7. **Effect of zoledronate on osteoblasts.** (A) Osteoblast numbers in zoledronate-treated and vehicle-treated groups. (B) Fold change of osteoblast surface per bone surface. (C) Fold change of osteoblasts per tissue area. (D) Fold change of osteoblasts per bone perimeter. The results are expressed as mean ± SD, n = 6. * $P < 0.05$, # $P < 0.05$ are considered to be statistically significant compared to representative control group, by Wilcoxon rank sum test. Dotted lines are set as 1 and express WT and TLR9 KO vehicle groups.

TLR9 deficiency did not have obvious effect on osteoclast formation upon zoledronate treatment

Here, we demonstrated that TLR9 deficiency did not affect the number of osteoclasts in vehicle-treated groups. Zoledronate decreased the number of osteoclasts in both WT and KO groups, but did not reach significance (Fig. 8A). Zoledronate significantly decreased the osteoclast surface per bone surface in both WT and KO groups ($p=0.0399$). There was no statistically significant difference between WT and KO groups upon zoledronate treatment (Fig. 8B). Zoledronate decreased the number of osteoclasts per tissue area, but did not reach significance (Fig. 8C). Zoledronate significantly decreased the number of osteoclasts per bone perimeter in both WT and KO groups compared to vehicle-treated groups ($p=0.0329$). There was no statistically significant difference between WT and KO groups upon zoledronate treatment (Fig. 8D).

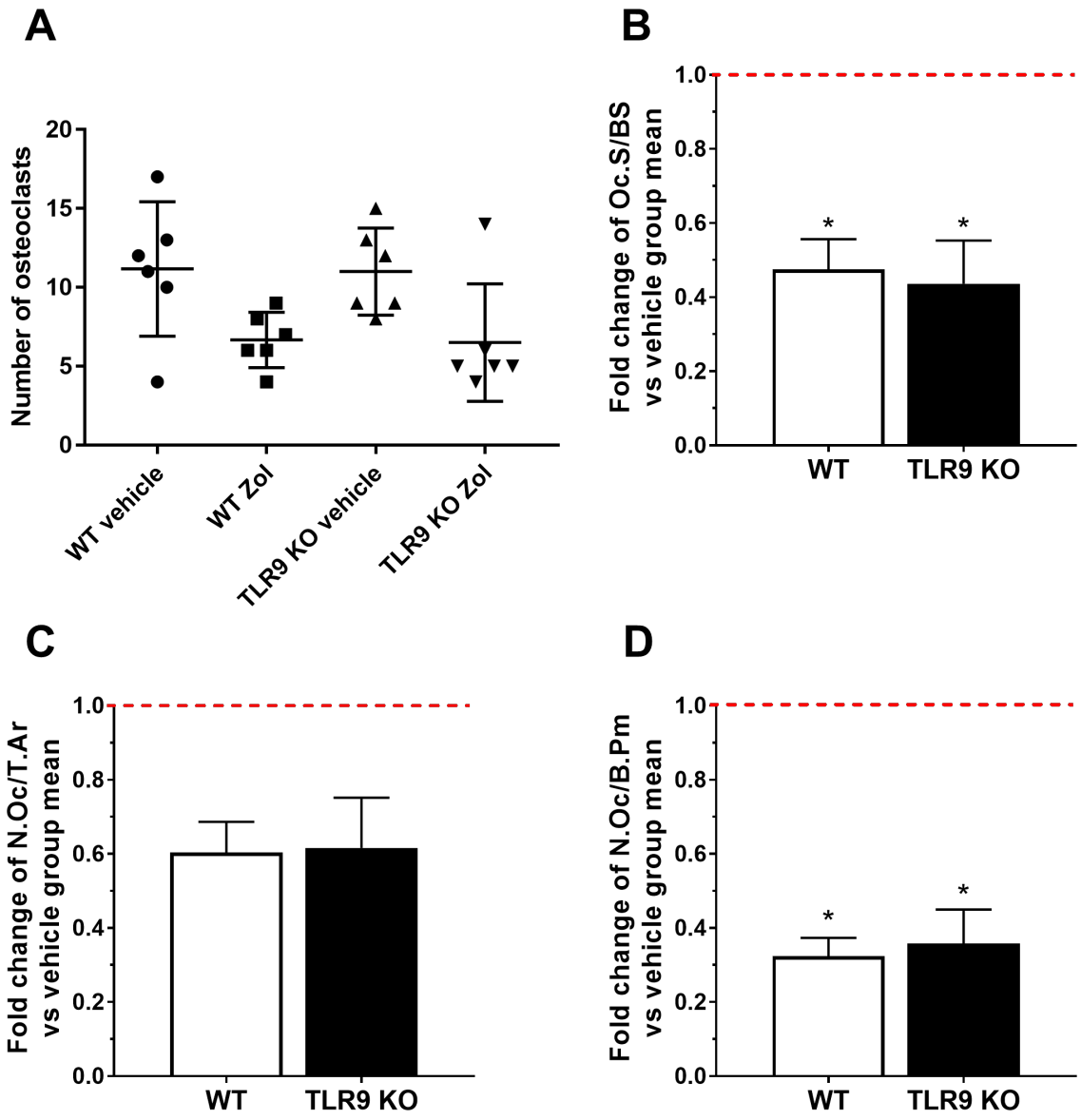

Figure 8. **Effect of zoledronate on osteoclasts in WT and KO groups.** (A) Osteoclast numbers in zoledronate-treated and vehicle-treated groups. (B) Fold change of osteoclast surface per bone surface. (C) Fold change of osteoclasts per tissue area. (D) Fold change of osteoclasts per bone perimeter. The results are expressed as mean ± SD, n = 6. * $P < 0.05$ is considered to be statistically significant compared to representative control group, by Wilcoxon rank sum test (B) or Tukey's HSD (D). Dotted lines are set as 1 and express WT and TLR9 KO vehicle groups.

Effect of TLR9 deficiency on cytokines after bisphosphonate treatment

Finally, we investigated the effects of TLR9 deficiency and zoledronate on cytokine expression. Cytokine concentrations (IFN-γ, IL-18, and IL-10) in plasma were analyzed with ProcartaPlex MultiPlex immunoassay. TLR9 deficiency increased IFN-γ level in vehicle group compared to the respective WT vehicle group. Controversially, after zoledronate treatment the level of IFN-γ decreased in TLR9 KO group compared to WT group. Zoledronate treatment increased the level of IFN-γ in WT group and decreased the level of IFN-γ in TLR9 KO group compared to respective vehicle-treated groups. The differences in IFN-γ levels were not statistically significant (Fig. 9A). Zoledronate increased the level of IL-10 in both WT and TLR9 KO groups compared to respective vehicle groups, but not significantly. TLR9 deficiency did not affect IL-10 concentration (Fig. 9B). TLR9 deficiency significantly increased the level of IL-18 in both vehicle and zoledronate-treated groups compared to the respective WT groups (Fig. 9C, $p=0.0028$).

These results indicate that TLR9 deficiency may increase the expression of IL-18.

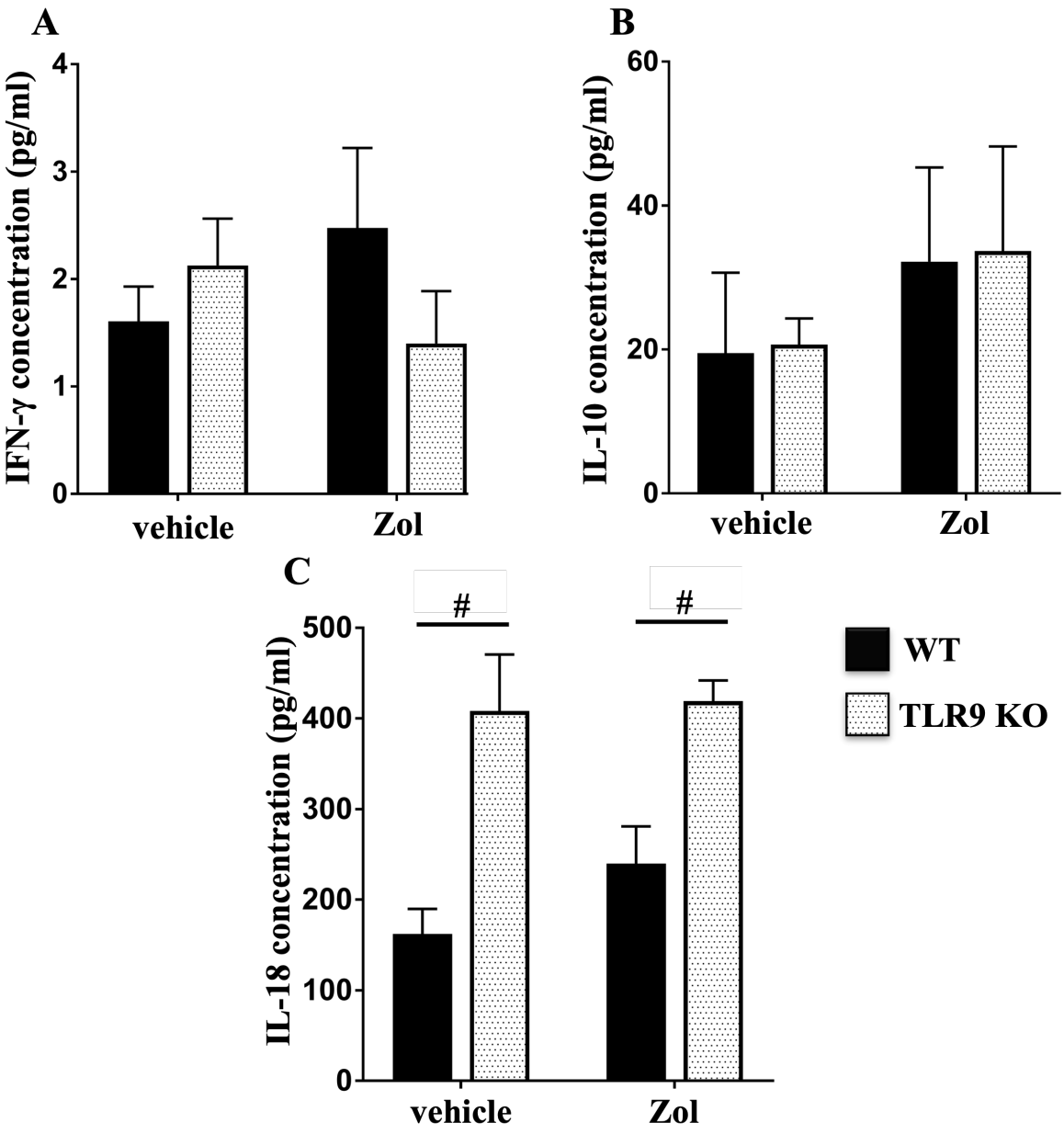

Figure 9. **Cytokine concentrations in vehicle-treated and zoledronate-treated WT and TLR9 KO groups.** (A) IFN-γ concentrations. (B) IL-10 concentrations. (C) IL-18 concentrations. The results are expressed as mean ± SD. # $P < 0.05$ is considered to be statistically significant compared to representative control group, by two-way ANOVA and Tukey's HSD.

DISCUSSION

TLR9 plays a role in bone formation. In previous studies, TLR9 stimulation in both osteoclast- and osteoblast-lineage cells has been shown to result in the induction and modulation of osteoclastogenesis(41,42). It has been shown that TLR9 stimulation increases osteoclast differentiation in RANKL-primed bone marrow-derived macrophages(41,43). However, it has also been shown that TLR9 stimulation of early osteoclast precursors inhibits their differentiation into mature osteoclasts(43–45). Zoledronate and other N-BPs inhibit osteoclastic bone resorption by inhibiting FPP synthase(21,22).

We observed that TLR9 deficiency prevented bone formation upon zoledronate treatment, since bone volume and number of osteoblasts were significantly lower in TLR9 KO groups (Figures 5 and 7). We also found that TLR9 deficiency increased IL-18 expression (Figure 9).

It has been observed previously that intraperitoneal injections of zoledronate cause splenomegaly in mice(46). Dose-dependent nephrotoxicity has also been reported both in rats and in humans upon zoledronate treatment(47,48). In particular, toxic acute tubular necrosis has been associated with zoledronate treatment(49). However, we found that zoledronate treatment had no significant effect on spleen weight or on the histology of renal tubules (Figures 3 and 4).

Several previous studies have demonstrated that the N-BPs zoledronate and pamidronate have an increasing effect on bone volume fraction *in vivo*(50–55). Zoledronate has also been shown to increase trabecular thickness and decrease trabecular separation *in vivo*(51,53–55). Our results show that zoledronate had an increasing effect on bone volume, bone volume fraction, and trabecular thickness, and a decreasing effect on trabecular separation (Figure 5).

The effect of zoledronate and other N-BPs on osteoclasts and osteoblasts has been investigated in several studies. N-BPs, such as zoledronate, alendronate, and pamidronate decrease the number of osteoclasts(33,51,56,57). One recent study showed that the number of osteoclasts increased upon pamidronate treatment(52). However, a few studies have reported that zoledronate had no significant effect on the number of osteoclasts(50,58). Our results show that zoledronate decreased the number of osteoclasts, but not significantly. Additionally, zoledronate significantly decreased the osteoclast surface per bone surface and the number of osteoclasts per bone perimeter (Figure 8). As stated before, the effect of TLR9 on osteoclasts depends on the stage of differentiation of osteoclasts. Whether the net effect of TLR9 on osteoclast formation is positive or negative remains unclear. Our results show that TLR9 had no significant effect on osteoclast parameters (Figure 8).

In vitro studies have revealed that zoledronate and other N-BPs increase osteoblastogenesis at low concentrations (10^{-9} to 10^{-6} M), and decrease osteoblastogenesis at concentrations higher than 10^{-5} M(33,54,57,59–63). However, there is a limited amount of evidence of the effects of zoledronate and other N-BPs on osteoblasts *in vivo*. A single dose of zoledronate had no effect on the number of osteoblasts, whereas repeated zoledronate treatment significantly decreased the number of osteoblasts(55). In one study, a local controlled delivery of zoledronate significantly increased the number of osteoblasts(51). Another research group got the result that alendronate significantly decreased the number of osteoblasts *in vivo*(38). Our results show that the number of osteoblasts increased significantly upon zoledronate treatment (Figure 7). It has been shown previously that TLR9 stimulation modulates the osteoclastogenic activity of osteoblasts(41,42). Our results show that TLR9 deficiency had a decreasing effect on the number of osteoblasts upon zoledronate treatment (Figure 7). The findings are supported by previous studies that have found that N-BPs increase osteoblastic activity(36–38).

The effect of TLR9 on cytokines has been addressed in several studies. It has been shown that in dendritic cells, TLR9 stimulation results in increased expression of several cytokines, including interferons, IL-6, IL-12 p40, and TNFα(2,64,65). In primary liver endothelial cells, TLR9 stimulation leads to the up-regulation of cytokines IL-1β and IL-18(4). We found that TLR9 deficiency increased the level of IL-18 and did not affect IL-10 concentration. Interestingly, TLR9 deficiency had an increasing effect on IFN-γ in vehicle groups and a decreasing effect upon zoledronate treatment (Figure 9).

It has been shown previously that N-BPs induce a pro-inflammatory response(28–31). Particularly, it has been observed that zoledronate administration leads to upregulation of cytokines IL-1β, IL-6, IL-17, IL-18, and TNFα(29,30,32). The effect of zoledronate on IFN-γ expression remains unclear. Zoledronate has also been shown to upregulate the expression of IFN-γ in peripheral blood mononuclear cells *in vitro*(66). However, in another study zoledronate had no effect on IFN-γ levels in humans *in vivo*(30). We found that zoledronate increased the level of IL-10. Zoledronate also slightly increased the level of IL-18. Interestingly, zoledronate increased the level of IFN-γ in WT group but had a decreasing effect on IFN-γ in TLR9 KO group (Figure 9).

CONCLUSIONS

According to our results, TLR9 increases the bone-strengthening effect of zoledronate, mainly by increasing osteoblastic activity. The findings may have clinical significance concerning the treatment of osteoporosis with N-BPs. Although osteoblastic activity is an important part of bone formation, other mechanisms explaining increased bone volume and trabecular bone formation in the presence of TLR9 are also possible and should be taken into account. These mechanisms include effects on osteoclast differentiation and on osteoclastogenic cytokines.

In conclusion, we found that TLR9 enhances the bone-strengthening effect of zoledronate. The relevance of the effects of TLR9 on osteoblasts and possible alternative mechanisms should be discovered in future research. We also found that TLR9 deficiency increases IL-18 expression in plasma. However, we found that TLR9 deficiency has no significant effect on IL-10 and IFN-γ concentrations. These results suggest that TLR9 deficiency may have a pro-inflammatory effect upon zoledronate treatment. The role of TLR9 in N-BP-induced inflammation remains an important subject of research.

REFERENCES

1. Akira S, Hemmi H. Recognition of pathogen-associated molecular patterns by TLR family. Immunol Lett. 2003 Jan 22;85(2):85–95.
2. Hemmi H, Takeuchi O, Kawai T, Kaisho T, Sato S, Sanjo H, et al. A Toll-like receptor recognizes bacterial DNA. Nat 2000 4086813. 2000 Dec 7;408(6813):740–5.
3. Latz E, Schoenemeyer A, Visintin A, Fitzgerald KA, Monks BG, Knetter CF, et al. TLR9 signals after translocating from the ER to CpG DNA in the lysosome. Nat Immunol 2004 52. 2004 Jan 11;5(2):190–8.
4. Imaeda AB, Watanabe A, Sohail MA, Mahmood S, Mohamadnejad M, Sutterwala FS, et al. Acetaminophen-induced hepatotoxicity in mice is dependent on Tlr9 and the Nalp3 inflammasome. J Clin Invest. 2009 Feb 2;119(2):305.
5. Sandholm J, Selander KS. Toll-Like Receptor 9 in Breast Cancer. Front Immunol. 2014 Jul 22;5:330.
6. Leifer CA, Kennedy MN, Mazzoni A, Lee C, Kruhlak MJ, Segal DM. TLR9 is Localized in the Endoplasmic Reticulum Prior to Stimulation. J Immunol. 2004 Jul 15;173(2):1179.

7. Bauer S, Kirschning CJ, Häcker H, Redecke V, Hausmann S, Akira S, et al. Human TLR9 confers responsiveness to bacterial DNA via species-specific CpG motif recognition. Proc Natl Acad Sci U S A. 2001 Jul 31;98(16):9237.

8. Suwarti S, Yamazaki T, Svetlana C, Hanagata N. Recognition of CpG oligodeoxynucleotides by human Toll-like receptor 9 and subsequent cytokine induction. Biochem Biophys Res Commun. 2013 Jan 25;430(4):1234–9.

9. Li Y, Berke IC, Modis Y. DNA binding to proteolytically activated TLR9 is sequence-independent and enhanced by DNA curvature. EMBO J. 2012 Feb 15;31(4):919.

10. Haas T, Schmitz F, Heit A, Wagner H. Sequence independent interferon-α induction by multimerized phosphodiester DNA depends on spatial regulation of Toll-like receptor-9 activation in plasmacytoid dendritic cells. Immunology. 2009 Feb;126(2):290.

11. Kindrachuk J, Potter JE, Brownlie R, Ficzycz AD, Griebel PJ, Mookherjee N, et al. Nucleic acids exert a sequence-independent cooperative effect on sequence-dependent activation of Toll-like receptor 9. J Biol Chem. 2007 May 11;282(19):13944–53.

12. Cai SY, Ouyang X, Chen Y, Soroka CJ, Wang J, Mennone A, et al. Bile acids initiate cholestatic liver injury by triggering a hepatocyte-specific inflammatory response. JCI Insight. 2017 Mar 9;2(5):e90780.

13. Tuomela J, Sandholm J, Karihtala P, Ilvesaro J, Vuopala KS, Kauppila JH, et al. Low TLR9 expression defines an aggressive subtype of triple-negative breast cancer. Breast Cancer Res Treat. 2012 Sep;135(2):481–93.

14. Kimmel DB. Mechanism of action, pharmacokinetic and pharmacodynamic profile, and clinical applications of nitrogen-containing bisphosphonates. J Dent Res. 2007 Nov 29;86(11):1022–33.

15. Coleman RE. Bisphosphonates: Clinical Experience. Oncologist. 2004;9 Suppl 4:14-27.

16. Frith JC, Mönkkönen J, Blackburn GM, Russell RGG, Rogers MJ. Clodronate and Liposome-Encapsulated Clodronate Are Metabolized to a Toxic ATP Analog, Adenosine 5′-(β,γ-Dichloromethylene) Triphosphate, by Mammalian Cells In Vitro. J Bone Miner Res. 1997 Sep 1;12(9):1358–67.

17. Mönkkönen H, Rogers MJ, Makkonen N, Niva S, Auriola S, Mönkkönen J. The cellular uptake and metabolism of clodronate in RAW 264 macrophages. Pharm Res. 2001;18(11):1550–5.

18. Frith JC, Mönkkönen J, Auriola S, Mönkkönen H, Rogers MJ. The molecular mechanism of action of the antiresorptive and antiinflammatory drug clodronate: Evidence for the formation in vivo of a metabolite that inhibits bone resorption and causes osteoclast and macrophage apoptosis. Arthritis Rheum. 2001 Sep;44(9):2201-10.

19. Van Beek E, Pieterman E, Cohen L, Löwik C, Papapoulos S. Farnesyl Pyrophosphate Synthase Is the Molecular Target of Nitrogen-Containing Bisphosphonates. Biochem Biophys Res Commun. 1999 Oct 14;264(1):108–11.

20. Bergstrom JD, Bostedor RG, Masarachia PJ, Reszka AA, Rodan G. Alendronate Is a Specific, Nanomolar Inhibitor of Farnesyl Diphosphate Synthase. Arch Biochem Biophys. 2000 Jan 1;373(1):231–41.

21. Rogers M. New insights into the molecular mechanisms of action of bisphosphonates. Curr Pharm Des. 2003 Mar 23;9(32):2643–58.

22. Van Beek E, Löwik C, Van Der Pluijm G, Papapoulos S. The Role of Geranylgeranylation in Bone Resorption and Its Suppression by Bisphosphonates in Fetal Bone Explants In Vitro: A Clue to the Mechanism of Action of Nitrogen-Containing Bisphosphonates. J Bone Miner Res. 1999 May 1;14(5):722–9.

23. Shipman CM, Croucher PI, Russell RG, Helfrich MH, Rogers MJ. The bisphosphonate incadronate (YM175) causes apoptosis of human myeloma cells in vitro by inhibiting the mevalonate pathway. Cancer Res. 1998 Dec 1;58(23):5294-7.

24. Virtanen SS, Väänänen HK, Härkönen PL, Lakkakorpi PT. Alendronate inhibits invasion of PC-3 prostate cancer cells by affecting the mevalonate pathway. Cancer Res. 2002 May 1;62(9):2708–14.

25. Coxon JP, Oades GM, Kirby RS, Colston KW. Zoledronic acid induces apoptosis and inhibits adhesion to mineralized matrix in prostate cancer cells via inhibition of protein prenylation. BJU Int. 2004 Jul 1;94(1):164–70.

26. Sawada K, Morishige K ichirou, Tahara M, Kawagishi R, Ikebuchi Y, Tasaka K, et al. Alendronate inhibits lysophosphatidic acid-induced migration of human ovarian cancer cells by attenuating the activation of rho. Cancer Res. 2002 Nov 1;62(21):6015–20.

27. Favier LA, Schulert GS. Mevalonate kinase deficiency: current perspectives. Appl Clin Genet. 2016 Jul 20;9:101.

28. Deng X, Tamai R, Endo Y, Kiyoura Y. Alendronate augments interleukin-1β release from macrophages infected with periodontal pathogenic bacteria through activation of caspase-1. Toxicol Appl Pharmacol. 2009 Feb 15;235(1):97–104.

29. Zhang Q, Yu W, Lee S, Xu Q, Naji A, Le AD. Bisphosphonate Induces Osteonecrosis of the Jaw in Diabetic Mice via NLRP3/Caspase-1-Dependent IL-1β Mechanism. J Bone Miner Res. 2015 Dec 1;30(12):2300.

30. Dicuonzo G, Vincenzi B, Santini D, Avvisati G, Rocci L, Battistoni F, et al. Fever After Zoledronic Acid Administration Is Due to Increase in TNF-a and IL-6. J Interf CYTOKINE Res. 2003;23:649–54.

31. Santini D, Fratto ME, Vincenzi B, Cesa A La, Dianzani C, Tonini G. Bisphosphonate effects in cancer and inflammatory diseases: In vitro and in vivo modulation of cytokine activities. BioDrugs. 2004 Aug 15;18(4):269–78.

32. Funayama H, Tashima I, Okada S, Ogawa T, Yagi H, Tada H, et al. Effects of Zoledronate on Local and Systemic Production of IL-1β, IL-18, and TNF-α in Mice and Augmentation by Lipopolysaccharide. Biol Pharm Bull. 2019;42(6):929–36.

33. Idris AI, Rojas J, Greig IR, Van't Hof RJ, Ralston SH. Aminobisphosphonates cause osteoblast apoptosis and inhibit bone nodule formation in vitro. Calcif Tissue Int. 2008 Mar 8;82(3):191–201.

34. Açil Y, Möller B, Niehoff P, Rachko K, Gassling V, Wiltfang J, et al. The cytotoxic effects of three different bisphosphonates in-vitro on human gingival fibroblasts, osteoblasts and osteogenic sarcoma cells. J Cranio-Maxillofacial Surg. 2012 Dec 1;40(8):e229–35.

35. Koyama C, Hirota M, Okamoto Y, Iwai T, Ogawa T, Hayakawa T, et al. A nitrogen-containing bisphosphonate inhibits osteoblast attachment and impairs bone healing in bone-compatible scaffold. J Mech Behav Biomed Mater. 2020 Apr 1;104:103635.

36. Plotkin LI, Weinstein RS, Parfitt AM, Roberson PK, Manolagas SC, Bellido T. Prevention of osteocyte and osteoblast apoptosis by bisphosphonates and calcitonin. J Clin Invest. 1999;104(10):1363.

37. Plotkin LI, Lezcano V, Thostenson J, Weinstein RS, Manolagas SC, Bellido T. Connexin 43 Is Required for the Anti-Apoptotic Effect of Bisphosphonates on Osteocytes and Osteoblasts In Vivo. J Bone Miner Res. 2008 Nov;23(11):1712.

38. Plotkin LI, Bivi N, Bellido T. A bisphosphonate that does not affect osteoclasts prevents osteoblast and osteocyte apoptosis and the loss of bone strength induced by glucocorticoids in mice. Bone. 2011 Jul;49(1):122.

39. Follet H, Li J, Phipps RJ, Hui S, Condon K, Burr DB. Risedronate and alendronate suppress osteocyte apoptosis following cyclic fatigue loading. Bone. 2007 Apr 1;40(4):1172–7.

40. Schindelin J, Arganda-Carreras I, Frise E, Kaynig V, Longair M, Pietzsch T, et al. Fiji - an Open Source platform for biological image analysis. Nat Methods. 2012 Jul;9(7):676–82.

41. Amcheslavsky A, Hemmi H, Akira S, Bar-Shavit Z. Differential Contribution of Osteoclast- and Osteoblast-Lineage Cells to CpG-Oligodeoxynucleotide (CpG-ODN) Modulation of Osteoclastogenesis. J Bone Miner Res. 2005 Sep 1;20(9):1692–9.

42. Zou W, Amcheslavsky A, Bar-Shavit Z. CpG Oligodeoxynucleotides Modulate the Osteoclastogenic Activity of Osteoblasts via Toll-like Receptor 9. J Biol Chem. 2003 May 9;278(19):16732–40.

43. Zou W, Schwartz H, Endres S, Hartmann G, Bar-Shavit Z. CpG oligonucleotides: novel regulators of osteoclast differentiation. FASEB J. 2002 Mar 1;16(3):274–82.

44. Amcheslavsky A, Bar-Shavit Z. Toll-like receptor 9 ligand blocks osteoclast differentiation through induction of phosphatase. J Bone Miner Res. 2007 Aug 1;22(8):1301–10.

45. Takami M, Kim N, Rho J, Choi Y. Stimulation by Toll-Like Receptors Inhibits Osteoclast Differentiation. J Immunol. 2002 Aug 1;169(3):1516–23.

46. Kiyama T, Okada S, Tanaka Y, Kim S, Bando K, Hasegawa M, et al. Inflammatory and Necrotic Effects of Minodronate, a Nitrogen-Containing Bisphosphonate, in Mice. Tohoku J Exp Med. 2013;230(3):141–9.

47. Pfister T, Atzpodien E, Bohrmann B, Bauss F. Acute Renal Effects of Intravenous Bisphosphonates in the Rat. Basic Clin Pharmacol Toxicol. 2005 Dec 1;97(6):374–81.

48. Chang JT, Green L, Beitz J. Renal Failure with the Use of Zoledronic Acid. N Engl J Med. 2003 Oct 23;349(17):1676-9; discussion 1676-9.

49. Markowitz GS, Fine PL, Stack JI, Kunis CL, Radhakrishnan J, Palecki W, et al. Toxic acute tubular necrosis following treatment with zoledronate (Zometa). Kidney Int. 2003 Jul 1;64(1):281–9.

50. Vermeer J, Renders G, Duin M van, Jansen I, Bakker L, Kroon S, et al. Bone-site-specific responses to zoledronic acid. Oral Dis. 2017 Jan 1;23(1):126–33.

51. Gou W, Wang X, Peng J, Lu Q, Wang Y, Wang A, et al. Controlled Delivery of Zoledronate Improved Bone Formation Locally In Vivo. PLoS One. 2014 Mar 11;9(3):e91317.

52. Morse A, McDonald MM, Mikulec K, Schindeler A, Munns CF, Little DG. Pretreatment with Pamidronate Decreases Bone Formation but Increases Callus Bone Volume in a Rat Closed Fracture Model. Calcif Tissue Int 2019 1062. 2019 Oct 1;106(2):172–9.

53. Brouwers JEM, Lambers FM, Gasser JA, Rietbergen B van, Huiskes R. Bone Degeneration and Recovery after Early and Late Bisphosphonate Treatment of Ovariectomized Wistar Rats Assessed by In Vivo Micro-Computed Tomography. Calcif Tissue Int. 2008 Mar;82(3):202.

54. Pozzi S, Vallet S, Mukherjee S, Cirstea D, Vaghela N, Santo L, et al. High-dose zoledronic acid impacts bone remodeling with effects on osteoblastic lineage and bone mechanical properties. Clin Cancer Res. 2009 Sep 15;15(18):5829–39.

55. Herrak P, Görtz B, Hayer S, Redlich K, Reiter E, Gasser J, et al. Zoledronic acid protects against local and systemic bone loss in tumor necrosis factor-mediated arthritis. Arthritis Rheum. 2004 Jul 1;50(7):2327–37.

56. Dong W, Qi M, Wang Y, Feng X, Liu H. Zoledronate and high glucose levels influence osteoclast differentiation and bone absorption via the AMPK pathway. Biochem Biophys Res Commun. 2018 Nov 10;505(4):1195–202.

57. Kellinsalmi M, Mönkkönen H, Mönkkönen J, Leskelä H-V, Parikka V, Hämäläinen M, et al. In vitro Comparison of Clodronate, Pamidronate and Zoledronic Acid Effects on Rat

Osteoclasts and Human Stem Cell-Derived Osteoblasts. Basic Clin Pharmacol Toxicol. 2005 Dec 1;97(6):382–91.

58. Amanat N, McDonald M, Godfrey C, Bilston L, Little D. Optimal Timing of a Single Dose of Zoledronic Acid to Increase Strength in Rat Fracture Repair. J Bone Miner Res. 2007 Jun 1;22(6):867–76.

59. Greiner S, Kadow-Romacker A, Lübberstedt M, Schmidmaier G, Wildemann B. The effect of zoledronic acid incorporated in a poly(D,L-lactide) implant coating on osteoblasts in vitro. J Biomed Mater Res - Part A. 2007 Mar 15;80(4):769–75.

60. Orriss IR, Key ML, Colston KW, Arnett TR. Inhibition of osteoblast function in vitro by aminobisphosphonates. J Cell Biochem. 2009 Jan 1;106(1):109–18.

61. Pan B, To LB, Farrugia AN, Findlay DM, Green J, Gronthos S, et al. The nitrogen-containing bisphosphonate, zoledronic acid, increases mineralisation of human bone-derived cells in vitro. Bone. 2004 Jan 1;34(1):112–23.

62. Xiong Y, Yang HJ, Feng J, Shi ZL, Wu LD. Effects of alendronate on the proliferation and osteogenic differentiation of MG-63 cells. J Int Med Res. 2009 Mar 1;37(2):407–16.

63. Im G Il, Qureshi SA, Kenney J, Rubash HE, Shanbhag AS. Osteoblast proliferation and maturation by bisphosphonates. Biomaterials. 2004 Aug 1;25(18):4105–15.

64. Sasai M, Linehan MM, Iwasaki A. Bifurcation of Toll-Like Receptor 9 Signaling by Adaptor Protein 3. Science. 2010 Sep 17;329(5998):1530.

65. Honda K, Ohba Y, Yanai H, Hegishi H, Mizutani T, Takaoka A, et al. Spatiotemporal regulation of MyD88–IRF-7 signalling for robust type-I interferon induction. Nat 2005 4347036. 2005 Apr 6;434(7036):1035–40.

66. Takimoto R, Suzawa T, Yamada A, Sasa K, Miyamoto Y, Yoshimura K, et al. Zoledronate promotes inflammatory cytokine expression in human CD14-positive monocytes among peripheral mononuclear cells in the presence of γδ T cells. Immunology. 2021 Mar 1;162(3):306–13.